



HAL
open science

Reactive liquid–liquid extraction of bio-based 3-hydroxypropionic acid using a biocompatible organic phase containing a tertiary amine: A model-based approach to elucidate dominant mechanisms

Pedro Arana-Agudelo, Marwen Moussa, Ioan-Cristian Trelea, Kevin Lachin, Violaine Athès

► To cite this version:

Pedro Arana-Agudelo, Marwen Moussa, Ioan-Cristian Trelea, Kevin Lachin, Violaine Athès. Reactive liquid–liquid extraction of bio-based 3-hydroxypropionic acid using a biocompatible organic phase containing a tertiary amine: A model-based approach to elucidate dominant mechanisms. *Separation and Purification Technology*, 2022, 294, pp.121184. 10.1016/j.seppur.2022.121184. hal-03663385

HAL Id: hal-03663385

<https://agroparistech.hal.science/hal-03663385>

Submitted on 10 May 2022

HAL is a multi-disciplinary open access archive for the deposit and dissemination of scientific research documents, whether they are published or not. The documents may come from teaching and research institutions in France or abroad, or from public or private research centers.

L'archive ouverte pluridisciplinaire **HAL**, est destinée au dépôt et à la diffusion de documents scientifiques de niveau recherche, publiés ou non, émanant des établissements d'enseignement et de recherche français ou étrangers, des laboratoires publics ou privés.

1 *Reactive liquid-liquid extraction of bio-based 3-hydroxypropionic acid using a*
2 *biocompatible organic phase containing a tertiary amine: a model-based approach to*
3 *elucidate dominant mechanisms*

4
5 Pedro Arana-Agudelo, Marwen Moussa, Ioan-Cristian Trelea, Kevin Lachin, Violaine Athès

6
7 Université Paris-Saclay, INRAE, AgroParisTech, UMR SayFood, F-91120, Palaiseau, France

8
9 Corresponding author: marwen.moussa@agroparistech.fr

10 DOI: 10.1016/j.seppur.2022.121184

11 **Abstract**

12 This work studies reactive liquid-liquid extraction of 3-hydroxypropionic acid (3-HP) from
13 aqueous solutions using a biocompatible organic phase consisting in N,N-
14 didodecylmethylamine (DDMA) (20% v/v) diluted in 1-dodecanol (40% v/v) and dodecane
15 (40% v/v). The objective was to propose an equilibrium model based on the law of mass
16 action accounting for the main phenomena occurring in the system. A set of equilibrium
17 extraction experiments was performed in the initial acid concentration range 0.0028 – 1 mol
18 L⁻¹ in order to determine the extraction yield, equilibrium pH and to collect infrared spectra of
19 the loaded organic phases. FT-IR spectra allowed to identify and elucidate the main
20 mechanisms of acid-amine interaction, which were taken into account in the model. The
21 formation of 1:1 acid-amine stoichiometry complex through ion-pairing was determined as
22 the dominant mechanism in all the concentration range. For initial acid concentrations above
23 0.11 mol L⁻¹, the formation of 2:1 acid-amine complexes through H-bonding of acid molecules
24 with 1:1 complexes was also observed and determined to be almost as important as ion-pair
25 formation at 1 mol L⁻¹. The presence of impurities in the organic phase was taken into
26 account by introducing a side reaction essential to represent low extraction yields and high
27 equilibrium pH values observed at low initial acid concentrations (< 0.02 mol L⁻¹). A global
28 sensitivity analysis of the model's parameters pointed out three concentration regions based
29 on the relative contribution of each phenomenon: (i) for initial acid concentrations below 0.02
30 mol L⁻¹, the main phenomena are 1:1 ion-pair formation and the side reaction; (ii) between
31 0.02 mol L⁻¹ and 0.11 mol L⁻¹, mainly 1:1 ion-pair formation; and (iii), for concentrations above
32 0.11 mol L⁻¹ both considered complexation reactions i.e., 1:1 ion-pair formation and 2:1 H-
33 bonding. The proposed model allowed thus to evaluate the relative importance of the
34 phenomena occurring in the system in all the studied acid concentration range.

35
36 Keywords: organic acids, N,N-didodecylmethylamine (DDMA), apparent amine basicity,
37 equilibrium modeling, infrared spectroscopy

38 **Nomenclature**

Abbreviations	Meaning	
3-HP	3-hydroxypropionic acid	
DDMA	N,N-didodecylmethylamine	
FT-IR	Fourier Transform Infrared spectroscopy	
MAE	Mean Absolute Error	
SE	Standard Error	
TOA	Trioctylamine	
Symbol	Definition	Unit
$[i]$	i -species concentration in aqueous phase	mol L ⁻¹
$[\bar{i}]$	i -species concentration in organic phase	mol L ⁻¹
Greek letters		
β	Apparent equilibrium constant	
δ	Bending vibrational mode	
φ	Organic phase diluents to total volume ratio	-
ν	Stretching vibrational mode	
K_a	3-HP dissociation constant	mol L ⁻¹
K_{11}	1:1 ion pair complex formation constant	L ² mol ⁻²
K_{21}	2:1 complex formation constant	L mol ⁻¹
K_{aq}	Side reaction constant	-
K_m	Partition coefficient	-
K_w	Water autoprotolysis constant	L ² mol ⁻²
$P_{o/w}$	Octanol / water partition coefficient	-
S	Sobol index	
Y	Extraction yield	%
Z	Loading ratio	mol mol ⁻¹
Subscripts/superscripts		
0	Initial concentration	
aq	Relative to the aqueous phase	
as	asymmetric stretch	
eq	Total concentration at the equilibrium	
exp	Experimental data	
hn	Half-neutralization point	
$HPLC$	Analytical concentration measured using High Performance Liquid Chromatography	
org	Relative to the organic phase	

<i>p</i>	Number of acid molecules in the complex
<i>s</i>	Symmetric stretch
<i>sim</i>	Simulated data
<i>t</i>	Total concentration
<i>T</i>	Total Sobol indices

39

40

41 **1. Introduction**

42

43 Due to growing concerns about climate change and the dependence on fossil
44 resources [1], there is an increasing interest in the substitution of crude oil derivatives
45 by bio-based products obtained from renewable feedstocks [2]. Historically, organic
46 acids have been widely used in industry. The bioeconomy context has reinforced the
47 interest in their production through biotechnological routes from renewable resources,
48 for the development of bio-based materials [3]. Carboxylic acid biological production
49 is inhibited by acid accumulation during the process, limiting both its productivity and
50 titer. The inhibition can be alleviated by the implementation, among other techniques,
51 of *In Situ* or In Stream Product Recovery (ISPR) processes. On the subject of
52 extractive production of carboxylic acids, reactive liquid-liquid extraction has been
53 extensively studied due to its high selectivity even at low acid titers, mild operation
54 conditions, the possibility of continuous extractant regeneration and its low energy
55 consumption [4,5].

56

57 Several extractants have been studied for the recovery of organic acids in literature.
58 Kertes and King [6] classified the different extractants into (i) carbon-bonded oxygen-
59 donor, (ii) phosphorous-bonded oxygen-donor and (iii) high molecular weight aliphatic
60 amines. Among the diversity of extractants suitable for this application, tertiary
61 aliphatic amines solubilized in organic solvents are the most common. Tertiary
62 amines are highly hydrophobic molecules that interact with the acid present in
63 aqueous phase through successive reversible complexation reactions at the liquid-
64 liquid interface. The distribution ratios that can be achieved using tertiary amines are
65 usually higher than those obtained with other extractants when the organic phase is
66 properly formulated [7]. As amines show poor solvating properties, the formulation of
67 organic phases generally includes an active diluent such as long-chain alcohols,
68 capable of strongly solvating the acid-amine complexes through polar interactions
69 (e.g. formation of H-bonds) [8].

70

71 3-hydroxypropionic acid (3-HP) emerged as one of the most promising chemical
72 building blocks for the production of acrylic acid, biopolymers, and other chemicals
73 with a wide range of applications in industry [9–11]. In this context, the interest in
74 microbial production of 3-HP has increased in the last years [12,13]. 3-HP recovery

75 from microorganisms culture broths is still challenging because of the hydrophilic
76 nature of this molecule ($\log P_{o/w} = -0.89$) and the low titers reached in the
77 process ($< 10\%$ w/w) due to low pH and acid inhibition [14]. This is why the
78 implementation of reactive liquid-liquid extraction shows encouraging prospects.

79
80 The main drawback of reactive liquid-liquid extraction as ISPR technique remains the
81 toxicity of the extraction phases in close contact with culture media. Recently, several
82 studies have been published on the screening and formulation of organic phases
83 accounting for the biocompatibility with some bacteria of the genus *Lactobacillus*
84 [15,16]. In spite of the identification of more biocompatible organic phases, most
85 experimental and equilibrium modeling studies so far focused on trioctylamine (TOA)
86 or the commercially available Alamine 336 (a blend of C₈ and C₁₀ trialkylamines) in
87 different mixtures of active and inert diluents, which are mostly deleterious for
88 microorganisms.

89
90 The objective of this work is thus to propose an equilibrium model of the extraction of
91 3-hydroxypropionic acid using a new formulation of organic phase that has been
92 identified from literature to be more biocompatible than other organic phases
93 employed for 3-HP extraction [15,17]. Among promising biocompatible organic
94 phases, we chose to focus on N,N-didodecylmethylamine (DDMA) diluted in a
95 mixture of 1-dodecanol and dodecane as active and inactive diluent, respectively,
96 according to the recent study of Sánchez-Castañeda et al. [15]. The authors found
97 that DDMA showed better performances than TOA in terms of distribution coefficient
98 as well as biocompatibility towards the natural 3-HP producer microorganism
99 *Lactobacillus reuteri*. They attributed better extraction performances to the reduction
100 of steric hindrance for reacting with acid molecules, while biocompatibility was linked
101 to more hydrophobic nature of DDMA. The inclusion of long chain aliphatic alcohols
102 as active diluents improved extraction performance. Nevertheless, depending on the
103 chain length, primary alcohols could increase toxicity. As was the case for
104 extractants, diluents' biocompatibility was found to be related to hydrophobicity,
105 longer carbon chains being less toxic. The inclusion of alkanes as inert diluents was
106 found to decrease extraction yield but was useful to further reduce toxicity, improving
107 mass transfer. Thus, the authors concluded that the organic phase containing DDMA

108 diluted in 1-dodecanol and dodecane presented the best trade-off between extraction
109 yield and biocompatibility.

110
111 In order to elucidate the underlying 3-HP extraction mechanisms, a set of extraction
112 equilibrium experiments was performed at different initial acid concentrations. Fourier
113 Transform Infrared spectroscopy (FT-IR) of loaded organic phases was employed as
114 a means to understand the nature of acid-amine interactions. In order to validate and
115 quantify the extraction mechanisms, a model built on the law of mass action,
116 considering different acid-amine interactions was developed and its parameters were
117 calibrated based on experimental data. The distribution of acid species in the organic
118 phase was thus studied. A global sensitivity analysis of the model was ultimately
119 performed through the estimation of main and total Sobol indices. The sensitivity
120 analysis quantified the importance of each parameter in different acid concentration
121 ranges and supported the discussion of the relative importance of the considered
122 mechanisms.

123

124 **2. Materials and Methods**

125 **2.1. Chemicals**

126

127 3-Hydroxypropionic acid (CAS number 503-66-2) was purchased from TCI-Europe
128 (Zwijndrecht, Belgium) as a 29.1% w/w solution in water. This solution was used to
129 prepare all the solutions of the studied concentration range. N,N-
130 didodecylmethylamine (DDMA, CAS number 2915-90-4, 98.1% purity) was purified
131 as detailed in 2.2 and then diluted in 1-dodecanol (CAS number 112-53-8, 99%
132 purity) and dodecane (CAS number 112-40-3, 99.5% purity), all three from TCI-
133 Europe. Sulfuric acid (CAS number 7664-93-9, 95%) was purchased from Sigma-
134 Aldrich (St. Louis, USA) and sodium hydroxide in aqueous solution (CAS number
135 1310-73-2, 35% w/w) from VWR Chemicals (Leuven, Belgium).

136

137 **2.2. Amine purification**

138 The commercial DDMA was purified by several steps of acid-base washing. Equal
139 volumes of commercial amine and aqueous H_2SO_4 0.1 mol L^{-1} were vigorously mixed
140 for 5 minutes and centrifuged during 1 h at $11\,000 g$ and 25°C . The organic phase
141 was then recovered and washed with equal volume of NaOH 0.3 mol L^{-1} before being

142 centrifuged at 11 000 *g* for 20 minutes. These steps were done twice. The resulting
143 organic phase was washed twice with Milli-Q ultrapure water and centrifuged for 1 h
144 at 11 000 *g*. The purified DDMA was diluted to 20% v/v (0.45 mol L⁻¹) in 1-dodecanol
145 (40% v/v) and dodecane (40% v/v) and used as organic extraction phase.

146

147 **2.3. Extraction equilibrium experiments**

148 Physical extraction experiments were performed by putting in contact 25 mL of
149 aqueous phases containing 3-HP in concentrations ranging from 0.0056 to 0.28 mol
150 L⁻¹ with equal volume of an organic phase consisting in 50% v/v 1-dodecanol and
151 50% v/v dodecane. The sample flask containing both phases was slightly mixed by
152 gentle shaking for 5 minutes and then settled to reach the equilibrium for 72 h at
153 25°C. After equilibration, acid concentration in the aqueous phase was analyzed by
154 HPLC and acid concentrations in organic phase were estimated through a mass
155 balance. The partition coefficient was determined as the slope of the regression line
156 of the graph of acid concentration in the organic phase versus acid concentration in
157 the aqueous phase (Figure A1). Reactive extraction was evaluated by performing the
158 same phase contacting protocol as for physical extraction. A volume of 2 mL of
159 aqueous 3-HP phases solutions ranging from 0.0028 to 1 mol L⁻¹ was put in contact
160 with equal volume of an organic phase containing 20% v/v purified DDMA, 40% v/v 1-
161 dodecanol and 40% v/v dodecane. Under these mild contacting conditions, the
162 formation of a stable emulsion difficult to separate was avoided. The time required to
163 reach equilibrium inside the flask was determined through a preliminary experiment
164 (not shown) and was found to be around 24 h. After reaching the equilibrium, the
165 aqueous phase was analyzed by HPLC and its equilibrium pH was measured using a
166 Mettler Toledo SevenCompact pH meter (Greisensee, Switzerland), equipped with a
167 Mettler Toledo InLab Viscous Pro-ISM probe (Greisensee, Switzerland). The loaded
168 extraction phase was recovered for FT-IR analysis. Each experiment was performed
169 in triplicate and the reported concentrations and FT-IR spectra are averages. The
170 extraction yield based on aqueous phase analysis was defined as Eq. (1):

171

$$Y_{exp} = \frac{[AH]_0^{HPLC} - [AH]_{eq}^{HPLC}}{[AH]_0^{HPLC}} \times 100\% \quad (1)$$

172

173 2.4. Analytical methods

174 The concentration of 3-hydroxypropionic acid in aqueous phases was measured by
 175 High-Performance Liquid Chromatography (HPLC) using a Biorad Aminex HPX-87H
 176 column (CA, USA). The mobile phase used was 0.5 mmol L⁻¹ H₂SO₄ at a flowrate of
 177 0.4 mL min⁻¹. The temperature was set at 65 °C. The samples were detected by a
 178 210 nm UV detector.

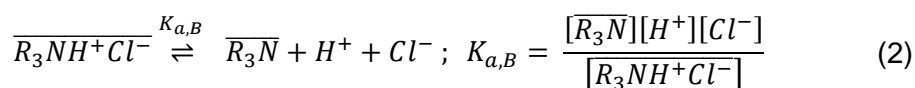
179 2.5. FT-IR spectra acquisition

181 A drop (~20 µL) of the liquid sample to analyze was enclosed between two CaF₂
 182 windows (ISP Optics, Riga, Latvia). IR spectra of the samples were recorded using a
 183 Nicolet Magna-IR 750 spectrometer (MA, USA) in the mid-IR region (wavenumbers
 184 between 800 and 4000 cm⁻¹) at ambient temperature. The resolution of the spectra
 185 was set to 2 cm⁻¹.

186
 187 Gaussian peak deconvolution was performed using the *Multiple peak fit* tool in Origin
 188 2021b software (OriginLab Corporation, MA, USA).

190 2.6. Amine basicity quantification

191 The amine basicity was estimated by determining the amine half-neutralization point
 192 as described by Canari and Eyal [18]. The cited method for determining the strength
 193 of highly hydrophobic amines was first introduced by Grinstead and Davis [19] as an
 194 analogy to acid-base equilibria in aqueous media. This method is based on the
 195 complete reaction of tertiary amines diluted in an organic phase after equilibration
 196 with aqueous hydrochloric acid, as expressed by Eq. (2).



198
 199 From Eq. (2) it is possible to define pK_{a,B} as Eq. (3):

$$200 pK_{a,B} = -\log\left(\frac{[\overline{R_3N}]}{[\overline{R_3NH^+Cl^-}]}\right) + \text{pH} - \log([Cl^-]) \quad (3)$$

201

202 The half-neutralization point corresponds to the point where half of the amine in the
 203 organic phase is neutralized by hydrochloric acid. Hence, at the half-neutralization
 204 point $[\overline{R_3N}]_{hn} = [\overline{R_3NH^+Cl^-}]_{hn}$, and $pK_{a,B}$ is given by Eq. (4):

205

$$pK_{a,B} = pH_{hn} - \log([Cl^-]) \quad (4)$$

206

207 Aiming to measure the pH at the half-neutralization point, a volume of 1 mL of
 208 organic phase was put in contact with HCl 1 mol L⁻¹ in an acid/amine molar ratio of
 209 1:1. After 72 h of contact, NaOH 0.5 mol L⁻¹ was added to the aqueous phase in an
 210 acid/base ratio of 2:1. The resulting pH of the aqueous phase recovered corresponds
 211 to pH_{hn} .

212

213 3. Theory

214

215 At the standard state (pure liquid at 25 °C), reactive liquid-liquid extraction of 3-HP
 216 using DDMA involves several physicochemical phenomena, namely physical
 217 partitioning, self-ionization of water, acid dissociation, reactive extraction by tertiary
 218 amine, electroneutrality and organic impurities impact. All these phenomena are
 219 considered below for modeling purposes.

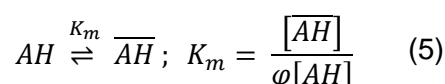
220

221 3.1. Physical partitioning

222

223 When aqueous 3-HP phases are in contact with an organic phase containing an
 224 extractant, almost all the acid transferred to the organic phase is extracted as acid-
 225 extractant complexes (reactive extraction). Nevertheless, a small part of the acid is
 226 present in the organic phase as a result of physical partitioning with the organic
 227 phase diluents, leading to the definition of the partition coefficient K_m introduced in
 228 Eq. (5).

229



230

231 where $[\overline{AH}]$ represents the concentration of total free acid in the organic phase,
 232 which is extracted by neat diluents, and $[AH]$ the total acid concentration in aqueous

233 phase. As the organic phase's total volume contains also the extractant, it is
 234 necessary to take into account the diluent's fraction φ expressed in Eq. (6).
 235

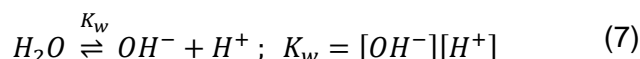
$$\varphi = \frac{V_{diluent}}{V_{org\ phase}} \quad (6)$$

236

237 3.2. Self-ionization of water

238

239 The equilibrium between hydronium and hydroxide ions in solution is determined by
 240 the auto-ionization constant of water. This equilibrium is presented in Eq. (7):
 241

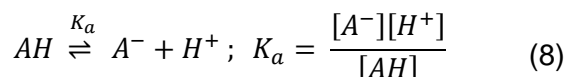


242

243 3.3. Acid dissociation

244

245 For a weak acid in an aqueous medium, the distribution of the undissociated and
 246 dissociated species is given by its dissociation constant K_a , presented in Eq. (8):



247

248 Based on the hydronium ion concentration (Eqs. (7-8)), pH in aqueous phases is
 249 defined as:

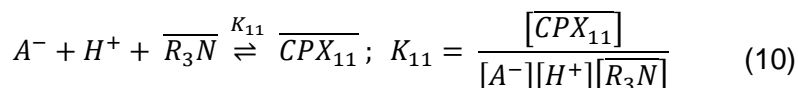
$$pH = -\log[H^+] \quad (9)$$

250

251 3.4. Complexation reactions by a tertiary amine

252

253 Reactive extraction of 3-HP is achieved through a set of reversible complexation
 254 reactions taking place between the acid in the aqueous phase and the tertiary amine
 255 in the organic phase. As reported by different authors ([20,21]), when the amine
 256 basicity is high enough to bind a proton, the formed cation interacts with the
 257 dissociated acid in aqueous phase to form a complex with 1:1 stoichiometry soluble
 258 in the organic phase. This mechanism is known as ion pair formation. The global
 259 reaction mechanism is presented in Eq. (10):



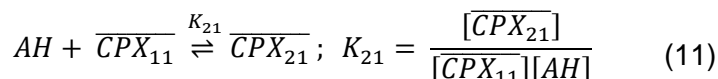
260

261 For simplification purposes, R_3 represents three generic alkyl groups, possibly
 262 different from each other. In the case of DDMA, $R_3 = R_2R'$, where R represents a
 263 dodecyl group and R' represents a methyl group.

264

265 At high initial acid concentrations, an undissociated acid molecule can interact with
 266 the 1:1 complex by hydrogen bonding thus forming a 2:1 complex.

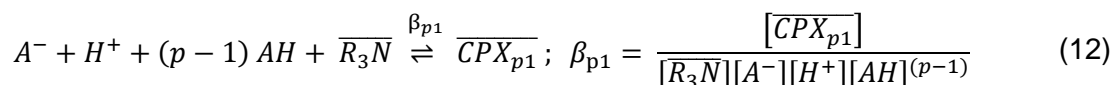
267



268

269 In the same manner as 2:1 complex formation, higher stoichiometry complexes could
 270 be formed through successive aggregation of acid molecules. This phenomenon
 271 depends on the acid nature, the extractant and the interaction between both of them.
 272 Considering that 1:1 complex is formed by ion-pairing, the global reaction of higher
 273 stoichiometry complexes can be described as Eq. (12):

274



275

276 where $\beta_{p1} = \prod_{n=1}^p K_{n1}$

277

278 Complexes containing more than one amine molecule can also be formed in some
 279 cases but are not considered in this work as this mechanism is likely to occur only for
 280 secondary amines [21].

281

282 The global extraction yield presented in Eq. (13) is defined as the ratio of all acid
 283 species in the organic phase and the initial acid concentration in the aqueous phase.

284

$$Y = \frac{[AH] + \sum_{n=1}^p n [\overline{CPX_{n1}}]}{[AH]_0} \frac{V_{org}}{V_{aq}} \times 100\% \quad (13)$$

285

286

287

3.5. Mass balances

288

289 The mass balances of the acid and the tertiary amine are given by Eqs (14) and (15)

290

$$[AH]_0 = [AH] + [A^-] + \frac{V_{org}}{V_{aq}} \left([AH] + \sum_{n=1}^p n [CPX_{n1}] \right) \quad (14)$$

291

$$[R_3N]_0 = [R_3N] + \sum_{n=1}^p [CPX_{n1}] \quad (15)$$

292

293 3.6. Amine loading ratio

294

295 The reactive extraction of the acid by a tertiary amine can be characterized using the
 296 loading ratio Z . The loading ratio of the extractant is defined as the ratio between the
 297 total concentration of acid in the organic phase (extracted by the amine) and the
 298 initial concentration of amine in the organic phase. The loading ratio is a function of
 299 the strength of the acid-amine interaction, the stoichiometry of the overall equilibrium
 300 reactions and the initial acid and extractant concentrations [22].

301

302 The general expression of the loading ratio is given by Eq. (16):

303

$$Z = \frac{\sum_{n=1}^p n [CPX_{n1}]}{[R_3N]_0} \quad (16)$$

304

305 When $p = 1$, i.e., ion-pair 1:1 complex formation, Z is defined as Eq. (17):

$$Z = \frac{[CPX_{11}]}{[R_3N]_0} \quad (17)$$

306

307 Combining Eq. (10), (15) and (17):

$$\frac{Z}{1-Z} = K_{11} [A^-] [H^+] \quad (18)$$

308

309 If reactive extraction follows ion-pair 1:1 complex formation, the plot of $Z/(1-Z)$
 310 versus $[A^-][H^+]$ yields a straight line with slope equal to K_{11} .

311

312 For the general case of the formation of higher stoichiometry complexes, if $[\overline{CPX}_{p1}] \gg$
 313 $[\overline{CPX}_{i1}]$; $i \neq p$, Z can be simplified as given in Eq. (19):
 314

$$Z \cong \frac{p [\overline{CPX}_{p1}]}{[R_3N]_0} \quad (19)$$

315
 316 Combining Eq. (12), (15) and (19):

$$\beta_{p1}[A^-][H^+][AH]^{(p-1)} \cong \frac{Z}{p-Z} \quad (20)$$

317
 318 Consequently, the plot of $Z/(p-Z)$ versus $[A^-][H^+][AH]^{(p-1)}$ is a straight line with
 319 slope $\beta_{p1} = \prod_{n=1}^p K_{n1}$, if the main assumption of predominance of $[\overline{CPX}_{p1}]$ is valid.
 320

321 3.7. Electroneutrality principle

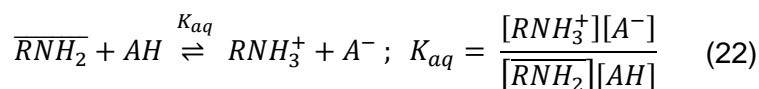
322
 323 Considering that there is no net charge in the aqueous phase, the sum of the
 324 concentration of positively charged species is equal to the sum of the concentrations
 325 of negatively charged species:
 326

$$[A^-] + [OH^-] = [H^+] \quad (21)$$

327 4. Modeling Reactive Liquid-Liquid Extraction

329 4.1. Organic impurities impact

330
 331 As a result of their synthesis process (alkylation of primary amines), commercial
 332 tertiary amines contain unreacted primary and secondary amines [23]. These lower
 333 amines, considered as impurities, are more soluble in water than tertiary amines and
 334 have an effect on the pH and the extraction yield. In order to model the effect of
 335 organic impurities on the extraction, a neutralization reaction was considered to occur
 336 between a pseudo-species $\overline{RNH_2}$, representing organic impurities (primary amines),
 337 and the undissociated acid. Impurities involved in the considered side reaction are
 338 solubilized into the aqueous phase. Eq (22) presents the side reaction:



339

340 The mass balance for impurities can be defined as Eq. (23):

$$[\overline{RNH_2}]_0 = [\overline{RNH_2}] + \frac{V_{aq}}{V_{org}} [RNH_3^+] \quad (23)$$

341
342 Given that a new positively charged species is introduced in the aqueous phase, the
343 electroneutrality principle is modified as stated in Eq. (24):

$$[A^-] + [OH^-] = [H^+] + [RNH_3^+] \quad (24)$$

345 346 4.2. Numerical solution of the mathematical models

347
348 Three different models of increasing complexity were compared in this study: firstly, a
349 model considering 1:1 complex formation and neglecting the presence of impurities,
350 secondly, the formation of a 2:1 complex was added to the first model, and finally, a
351 model including 1:1 and 2:1 complexes and the side reaction. Table 1. presents the
352 model equations, their parameters and their calibration datasets.

353
354 **Table 1.** Definition of the three considered models.

	Model	Equations	Parameters	Calibration datasets
1	1:1 stoichiometry model ($p = 1$) without impurities	(5), (7)-(8), (10), (14)-(15), (21)	K_{11}	Extraction yield
2	1:1 stoichiometry model ($p = 1$) + 2:1 stoichiometry model ($p = 2$) without impurities	(5), (7)-(8), (10)-(11), (14)-(15), (21)	K_{11}, K_{21}	Extraction yield
3	1:1 stoichiometry model ($p = 1$) + 2:1 stoichiometry model ($p = 2$) including impurities	(5), (7)-(8), (10)-(11), (14)-(15), (22)-(24)	K_{11}, K_{21}, K_{aq} and $[\overline{RH_2N}]_0$	Extraction yield Equilibrium pH

355
356 The parameters of models 1 and 2 were calibrated using the extraction yield
357 measured in the experimental section, by minimizing the difference between
358 measured and calculated values in the least-squares sense. For model 3, measured
359 equilibrium pH was also included as a calibration data set because one of the main

360 consequences of the side reaction was pH increase, compared to the theoretical
 361 values without impurities. The values of the two experimental datasets were divided
 362 by their respective ranges of variation in order to obtain values of similar order of
 363 magnitude suitable for simultaneous use in parameter calibration. Given that the
 364 correlation between K_{aq} and $[\overline{RH_2N}]_0$ was greater than 98%, it was not possible to
 365 estimate the two parameters simultaneously. For this reason, an external loop was
 366 implemented to make $[\overline{RH_2N}]_0$ vary between 0.5 and 5 mmol L⁻¹. For each fixed
 367 $[\overline{RH_2N}]_0$, parameters K_{11} , K_{12} and K_{aq} were determined. The combination of
 368 parameters giving the best fit was selected among the solutions significantly different
 369 from zero (i.e. zero was not included in the 95% confidence interval of either
 370 parameter).

371
 372 The goodness of fit of the proposed models has been evaluated using the mean
 373 absolute error (MAE), defined as Eq. (25)

$$MAE = \frac{1}{N} \sum_{k=1}^N |y_{exp} - y_{sim}| \quad (25)$$

374 where N is the number of experimental points, y_{exp} are the observed values and y_{sim}
 375 the predicted values.

376
 377 MATLAB R2020b (The MathWorks Inc., Natick, MA), equipped with Statistics and
 378 Optimization toolboxes was used for numerical calculations. For each model, the
 379 systems of nonlinear equations listed in Table 1 were solved with the 'trust region'
 380 algorithm implemented in the *fsolve* function. The *nlinfit* function implementing the
 381 Levenberg-Marquardt algorithm was used to solve the nonlinear least-squares
 382 problem for parameter estimation. The values of the fixed parameters for calculations
 383 are listed in Table 2.

384

385 **Table 2.** Fixed parameters for calculations

Parameter	Value	Unit	Present in Eq.
φ	0.8	-	(5)-(6), (13)-(14)
$K_a = 10^{-pK_a^*}$	3.09×10^{-5}	mol L ⁻¹	(8)
K_w	10^{-14}	L ² mol ⁻²	(7)
K_m^{**}	0.004	-	(5)

$[\overline{R_3N}]_0$	0.45	mol L ⁻¹	(15)-(17), (19)
V_{aq}	2×10^{-3}	L	(14), (23)
V_{org}	2×10^{-3}	L	(14), (23)

386 * Taken from [24]

387 ** Described in sec. 2.3 (Figure A1 in appendices).

388

389 4.3. Sensitivity analysis

390

391 Global Sensitivity Analysis was performed through the estimation of Sobol indices as
 392 described by Jansen [25] and Saltelli et al. [25]. For each initial acid concentration,
 393 the model was solved $N = 5 \times 10^4$ times with random parameter sets drawn from a
 394 normal distribution with standard deviation equal to 10 % of the mean estimated
 395 value of each parameter. Confidence intervals for Sobol indices were estimated using
 396 the bootstrap method.

397

398 5. Results and discussion

399

400 5.1. Experimental results: extraction yield and equilibrium pH

401

402 Table 3 and Figure 1 present the experimental yield, the observed equilibrium pH and
 403 loading ratios obtained from the equilibrium experiments described in section 2.3.

404

405 **Table 3.** Experimental equilibrium results

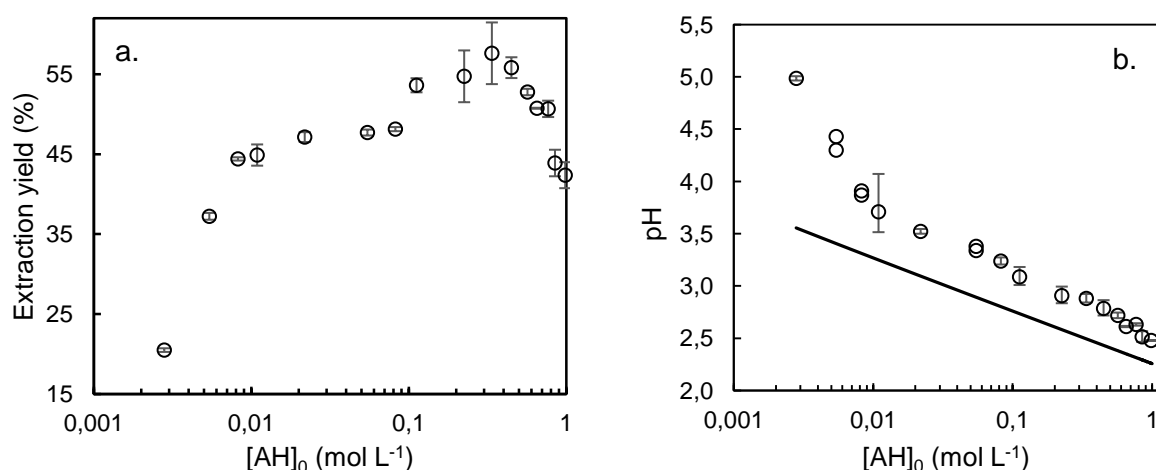
Initial acid concentration (mol L ⁻¹)	Extraction yield (%)	Equilibrium pH (-)	Loading ratio (mol mol ⁻¹)
0.0028	20.50	4.99	0.003
0.0054	37.23	4.36	0.008
0.0082	44.41	3.89	0.012
0.011	44.90	3.71	0.015
0.022	47.15	3.52	0.027
0.054	47.71	3.36	0.062
0.082	48.14	3.24	0.092
0.11	53.62	3.09	0.138
0.22	54.75	2.91	0.278
0.34	57.63	2.88	0.437

0.45	55.83	2.79	0.561
0.57	52.78	2.72	0.670
0.65	50.75	2.61	0.739
0.77	50.68	2.63	0.868
0.85	43.90	2.51	0.830
1.0	42.38	2.48	0.929

406

407 The extraction yield measured experimentally varied between 40% to 60% in all the
 408 studied concentration range except for concentrations lower than 0.008 mol L^{-1} , for
 409 which the observed yield is lower. This behavior has already been observed by some
 410 authors [27,28] and is generally related to the presence of impurities originated in
 411 commercial tertiary amines synthesis process. Impurities consist mainly in traces of
 412 primary amines as mentioned previously. Primary amines are less hydrophobic than
 413 tertiary amines (e.g. $\text{Log } P_{o/w} = 3.06$ for octylamine and $\text{Log } P_{o/w} = 10.94$ for TOA)
 414 and have a negative impact on the extraction performance by reacting with the acid
 415 in the aqueous phase. The availability of acid molecules to reactive extraction into the
 416 organic phase is thus decreased and its effect is especially noticeable at acid
 417 concentrations low enough to be comparable to the concentration of primary amines
 418 in the organic phase.

419



420 **Figure 1.** Experimental results as a function of initial 3-HP concentration
 421 a. Extraction yield, b. Equilibrium pH: experimental (symbols), theoretical (solid line).
 422 Error bars represent standard deviation
 423

424 This problem was illustrated by Kaur and Elst [27] by studying the reactive extraction
 425 of itaconic acid with several amines in many diluents. They reported that the most

426 effective extractants were the most hydrophobic ones. Inversely, the less
427 hydrophobic extractants showed poor extraction yields. As an example of this, those
428 authors found that the distribution ratio obtained using TOA in 1-decanol was almost
429 8 times higher than that using octylamine in the same diluent. These results were
430 attributed to the partial solubility of primary amines in the aqueous phase that
431 decreased their availability for acid extraction into the organic phase. Chemarin et al.
432 [28] obtained similar results for 3-HP extraction using TOA diluted in 1-decanol. They
433 found that in presence of octylamine in the organic phase at concentrations near 2
434 mmol L⁻¹, the extraction yield of 3-HP decreased from 70% to 10% for initial acid
435 concentrations lower than 0.1 mol L⁻¹. They proposed the acid-base purification
436 protocol presented in 2.2 and obtained a purified TOA containing less than 0.06
437 mmol L⁻¹ octylamine. The organic phase prepared using purified TOA showed no
438 decrease in extraction yield at lower acid concentrations. In the present study,
439 although DDMA was purified using the same protocol, the decrease in the extraction
440 yield was still observed at lower acid concentrations, suggesting that DDMA
441 purification was not optimal. Therefore, further studies need to be conducted to
442 precisely quantify the impurities in commercial DDMA aiming to design a more
443 adapted purification protocol.

444
445 The transfer of amine impurities to the aqueous phase also had an effect on the
446 equilibrium pH [29]. It can be observed that experimental pH measured at equilibrium
447 is indeed systematically higher than the theoretical pH estimated considering the 3-
448 HP concentration at equilibrium measured by HPLC (Figure 1b). The discrepancy is
449 especially high for acid concentrations below 0.008 mol L⁻¹.

450
451 In the range 0.08 mol L⁻¹ – 0.11 mol L⁻¹ the extraction yield seemed to reach a
452 plateau and increased again for $[AH]_0 > 0.11$ mol L⁻¹ with a maximum reached at
453 0.45 mol L⁻¹ (Figure 1a). This behavior could indicate that the reactive extraction in all
454 the studied range is the combination of different acid-amine interactions. When initial
455 acid concentrations are high enough ($Z > 0.5$), which corresponds to $[AH]_0$ higher or
456 equal to 0.45 mol L⁻¹ (Table 3), it is considered that more than one acid molecule is
457 complexed by the amine [30].

458

5.2. Nature of 3-HP-DDMA complex: an FT-IR spectroscopy study

459
460

461 In order to gain insights into the interactions between 3-HP molecules and amine in
462 the organic phase, several IR spectra were recorded. This section presents the
463 analysis of the FT-IR spectra of loaded extraction phases and results are further used
464 to support the mechanistic model of reactive liquid-liquid extraction of 3-HP using
465 DDMA in 1-dodecanol/dodecane. FT-IR spectra of different compounds used in this
466 study are presented in the appendices section.

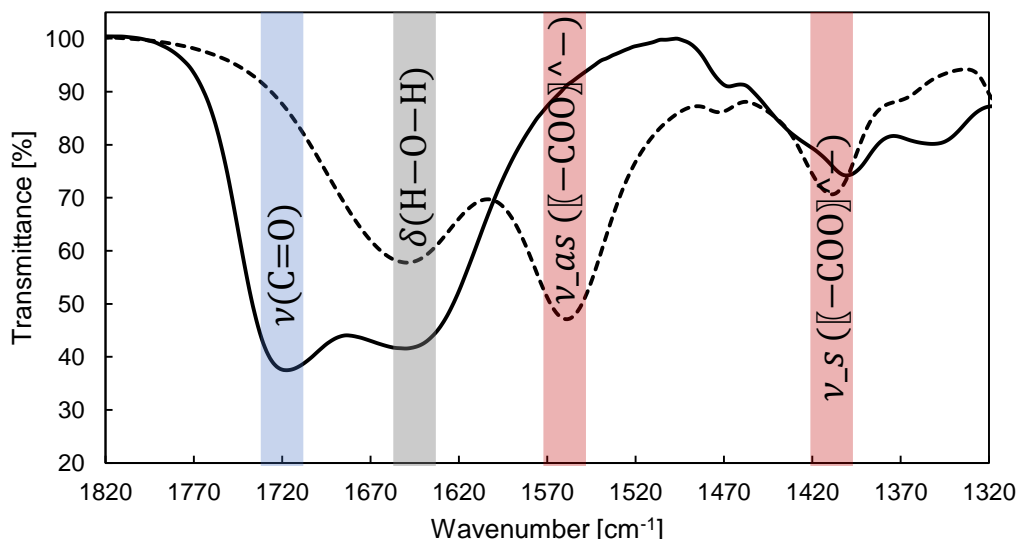
467

5.2.1. Organic acids characteristic IR bands

468
469

470 The spectral analysis of samples containing organic acids is particularly interesting in
471 the region $1100 - 1800 \text{ cm}^{-1}$ in which several carbonyl/carboxyl characteristic bands
472 of organic acids appear. As an example, Figure 2 presents FT-IR spectra of
473 commercial 3-HP aqueous acid and the same product neutralized with NaOH. pH of
474 the commercial 3-HP solution (3.2 mol L^{-1}) is about 2.0, consequently more than 99%
475 of the acid is in its undissociated form (estimated using Equation (8)). This product
476 showed a strong absorption peak at about 1720 cm^{-1} . The region comprising $1700 -$
477 1780 cm^{-1} corresponds to carbonyl stretch ($\nu(\text{C} = \text{O})$) in a carboxyl functional group
478 and has been extensively linked to the presence of undissociated forms of organic
479 acids [31]. When this region is present at lower wavenumbers ($1700 - 1720 \text{ cm}^{-1}$),
480 carbonyl groups are considered to be involved in hydrogen bonds. In certain cases,
481 they are associated to acid molecules forming cyclic dimers although cyclization has
482 not been yet proved by means of FT-IR data [32].

483



484
 485 **Figure 2.** FT-IR spectra of 3-HP in solution (3.2 mol L⁻¹)
 486 Commercial product (solid line), Commercial product neutralized with NaOH (dashed line)
 487

488 Regarding neutralized 3-HP (pH = 7, more than 99% dissociated), spectra lack a
 489 peak in the 1700 – 1720 cm⁻¹ region. Instead, a peak in the region 1550 – 1620 cm⁻¹
 490 appeared. In this case, the peak at about 1565 cm⁻¹ is assigned to the asymmetric
 491 stretch of the carboxylate group ($\nu_{as}(\text{COO}^-)$) and hence attributed to the presence of
 492 dissociated acid molecules [31]. A common peak between the two solutions could be
 493 found at about 1650 cm⁻¹ and is related to the bending of water molecules in the
 494 sample ($\delta(\text{H} - \text{O} - \text{H})$).

495

496 5.2.2. Loaded organic phases

497

498 In the light of the previously described absorption bands, a similar analysis was done
 499 for the loaded extraction phases aiming to elucidate the nature of the acid-amine
 500 interaction. FT-IR spectra of some loaded organic phases are presented in Figure 3.
 501 As it can be observed, all the spectra of loaded extraction phases present a peak at
 502 1571 cm⁻¹. This indicates the presence of the acid in its dissociated form and thus
 503 that the acid forms an ion-pair with the amine in the organic phase. This mechanism
 504 has been reported to be mostly dependent on the basicity (strength) of the extractant
 505 in the diluents, the dissociation constant of the acid and its hydrophobicity (for 3-HP,
 506 $\text{p}K_a = 4.51$, $\log P_{o/w} = -0.89$) [33].

507

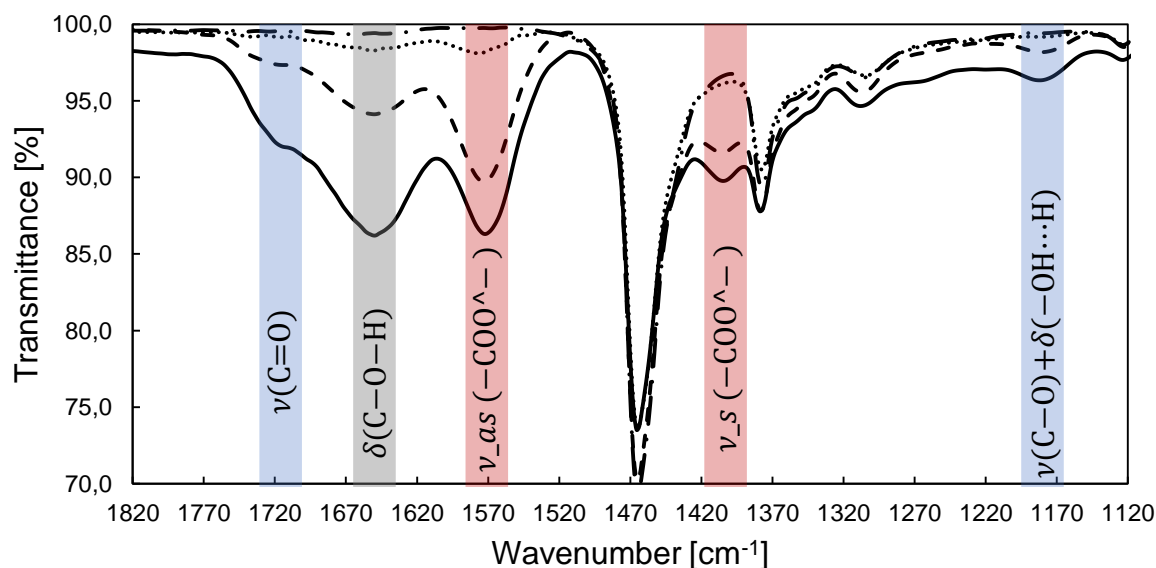


Figure 3. FT-IR spectra of organic extraction phases after prior equilibration with aqueous 3-HP solutions at different initial concentrations. $[AH]_0$: 0.01 mol L⁻¹ (dashdotted line), 0.11 mol L⁻¹ (dotted line), 0.55 mol L⁻¹ (dashed line), 1 mol L⁻¹ (solid line)

508
509
510
511
512
513

514 Due to the difficulty of estimating acid-base properties of water-insoluble tertiary
515 amines diluted in organic phases, it is convenient to define an apparent basicity with
516 respect to the equilibrium with protons in the aqueous phase. The apparent basicity
517 of a given amine in given diluents depends on amine properties (substituents, steric
518 hindrance), diluents' properties (polarity, proton donor or acceptor) and the extracted
519 acid [18]. Canari and Eyal [34] proposed an equilibrium constant $pK_{a,B}$ of the reaction
520 of the tertiary amine with HCl (section 2.6). Those authors stated that for amines with
521 higher or similar basicity than the conjugated base of the acid to extract ($pK_{a,B} \geq$
522 pK_a), ion-pairing is the predominant extraction mechanism.

523 The value of $pK_{a,B}$ measured for the organic phase used in this study was found to
524 be equal to 6.42 ± 0.08 . According to these results, DDMA (20% v/v) in 1-dodecanol
525 (40% v/v) and dodecane (40% v/v) is a stronger base than the conjugate base of 3-
526 HP in the aqueous phase. The amine is strong enough to bind a proton and the
527 dissociated acid form is therefore extracted in order to keep electroneutrality in the
528 organic phase. The presence of a polar diluent, especially a protic solvent such as 1-
529 dodecanol, plays an essential role in this mechanism by facilitating the solvation of
530 ion-pairs in the organic phase by polar interactions [33].

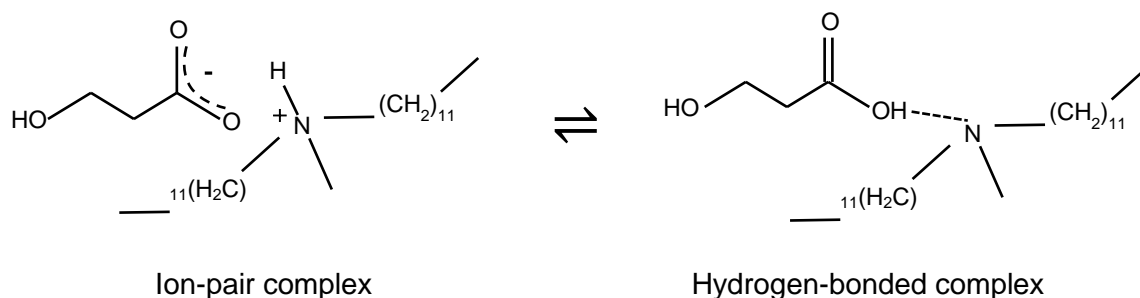
531 Recently, Chemarin et al [35] proposed this mechanism for 3-HP extraction based on
532 FT-IR data obtained using TOA in 1-decanol. Ion-pair formation has been widely
533 studied for several organic acids using different tertiary amines [36–38].

534 For initial acid concentrations higher than 0.11 mol L^{-1} , spectra of loaded organic
535 phases show a shoulder at about 1716 cm^{-1} . The apparition of this peak indicates the
536 presence of the undissociated acid form in the organic phase, more particularly,
537 carboxyl groups participating in H-bonds. Different explanations of this phenomenon
538 can be formulated: (i) the presence of free acid extracted by physical partitioning, (ii)
539 the existence of a tautomeric equilibrium between the ionic complex and a hydrogen-
540 bonded form of this complex, and (iii) the formation of high stoichiometry complexes.

541
542 Concerning hypothesis (i), the presence of free acid molecules in the organic phase
543 can be neglected due to the low partition coefficient of 3-HP in the organic phase
544 diluents ($K_m = 0.004$). In the studied concentration range ($0.0028 - 1 \text{ mol L}^{-1}$), the
545 acid extracted by physical partitioning is so low that it is undetectable by FT-IR.

546
547 Regarding hypothesis (ii), the existence of an equilibrium between a complex formed
548 by proton transfer and a molecular complex formed by hydrogen-bonding (see Figure
549 4) have been reported to happen in several acid-amine couples in different organic
550 phases [21,39,40]. Gusakova et al. [41] recorded spectra from an equimolar mixture
551 of isobutyric acid and triethylamine diluted in C_2Cl_4 . They observed a decrease of the
552 $\nu(\text{C}=\text{O})$ band and an increase of $\nu_{as}(-\text{COO}^-)$ proportional to the addition of
553 methanol (a polar and protic solvent). Hence, they concluded that tautomeric
554 equilibrium is highly dependent on the diluents, and it is mostly shifted to the ion-pair
555 form in presence of a polar solvent. These observations were also validated by the
556 same authors using isobutyric acid in dimethyl sulfoxide and acetonitrile, both polar
557 solvents. In this study, the presence of 1-dodecanol as a polar and protic diluent
558 (40% v/v) would shift the equilibrium showed in Figure 4 to the ion-pair form of the
559 complex.

560

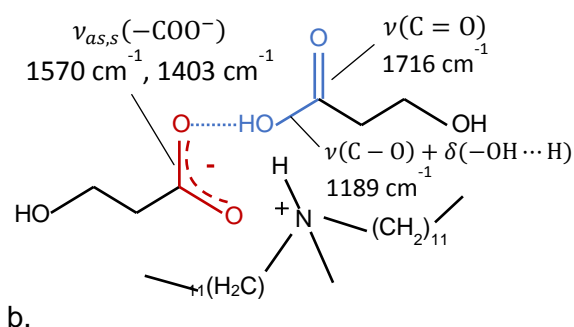
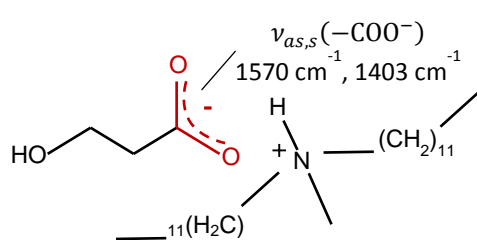


561 **Figure 4.** Tautomeric equilibrium of ionic and molecular 1:1 acid-amine complexes.

562
 563 As discussed previously, hypothesis (i) and (ii) are unlikely to occur, consequently,
 564 the apparition of the shoulder at $\sim 1716\text{ cm}^{-1}$ can be attributed to hypothesis (iii), i.e.,
 565 to the aggregation of undissociated acid molecules to the ion-pair complex through
 566 hydrogen bonding [42]. This seems to be in agreement with another phenomenon
 567 observed in spectra of loaded organic phases (Figure 3) for $[AH]_0 > 0.11\text{ mol L}^{-1}$: the
 568 apparition of a C – O bond stretch band ($\nu(\text{C} - \text{O})$) coupled with the scissoring of a
 569 hydrogen-bonded hydroxyl group ($\delta(-\text{OH} \cdots \text{O})$) at 1189 cm^{-1} [43]. The ratio between
 570 the surface of the $\nu(\text{C} = \text{O})$ band at 1716 cm^{-1} and $\nu(-\text{COO}^-)$ that at 1570 cm^{-1}
 571 decreases while increasing initial concentration of 3-HP. For this reason, the
 572 formation of high stoichiometry complexes is considered to gain importance with
 573 respect to 1:1 ion-pair formation at higher acid concentrations. The structure of the
 574 different acid-amine complexes considered is presented in Figure 5.

575

a.



b.

576 **Figure 5.** Proposed structures for acid-amine complexes and their characteristic IR
 577 bands

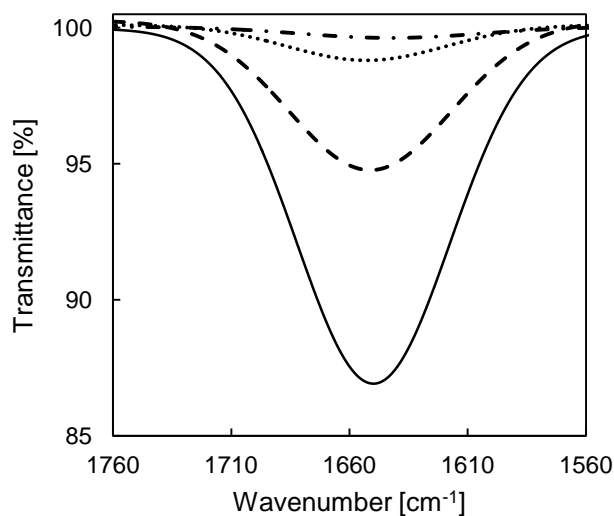
578 a. 1:1 complex, b. 2:1 complex

579

580
581
582
583
584
585
586
587
588
589
590
591
592
593
594

5.2.3. Water co-extraction

All the loaded organic phases showed the characteristic peak of bending of water molecules at 1650 cm^{-1} . Tamada and King [44] observed water co-extraction in a set of reactive extraction experiments of several mono and dicarboxylic acids using Alamine 336 in different active diluents. They reported that this phenomenon was highly dependent on the solubility of free water molecules in active diluents. They also observed that monocarboxylic acids such as lactic and acetic acid carried less water than dicarboxylic acids, inferring that water molecules were tightly bound to the carboxylate part of organic acids. In this work, when the organic phase was priorly equilibrated with pure water, the observed water band is negligible (Figure 6) and it increases while increasing the initial acid concentration. Therefore, the presence of the water band in loaded organic phases is due to the co-extraction of water molecules bound to acid-amine complexes.



595
596
597
598
599
600
601
602
603
604
605

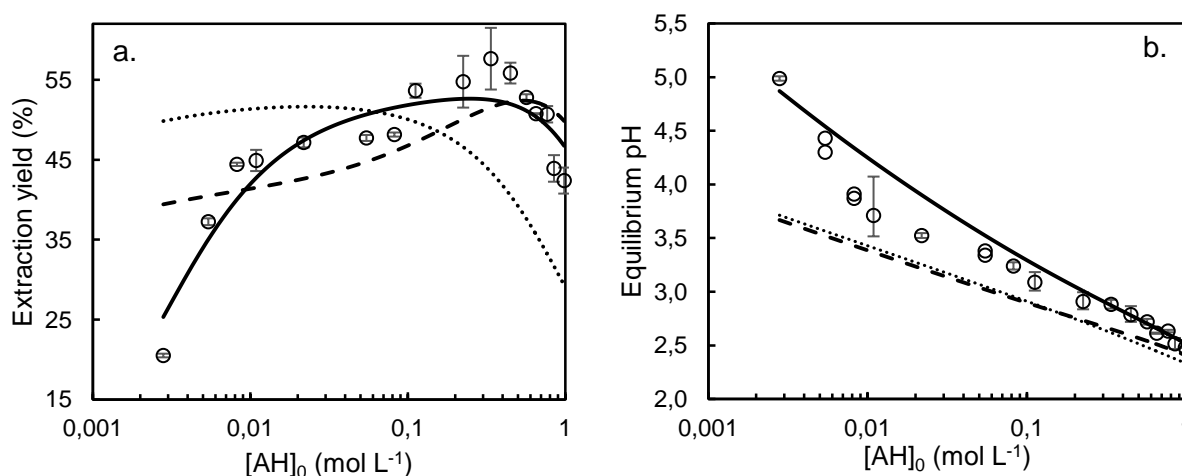
Figure 6. Deconvoluted water bands in loaded organic phases
Pure water (dashdotted line), organic phases after being equilibrated with 3-HP
solutions:
 0.11 mol L^{-1} (dotted line), 0.55 mol L^{-1} (dashed line), 1 mol L^{-1} (solid line)

In Figure 6, a deconvolution of the peaks showed in Figure 3 was done for the sake of better data visualization than in the case of the overlapping peaks.

5.3. Modeling results

606 Figure 7 shows the predicted extraction yield and equilibrium pH for the three
607 models,
608 calibrated based on experimental data. Table 4 presents the estimated parameters of
609 each model. It appears that model 1 predicts a slight increase of the extraction yield
610 while increasing initial acid concentrations until 0.02 mol L^{-1} . For higher
611 concentrations, amine becomes the limiting reactant, and consequently, a strong
612 decline is observed. Recall that Model 1 includes only the 1:1 acid-amine complex
613 formation, and accordingly is unable to predict the behavior observed for acid
614 concentrations exceeding 0.1 mol L^{-1} (increase in yield) and below 0.08 mol L^{-1}
615 (strong yield decrease and high equilibrium pH). Model 1 shows thus poor accuracy
616 for predictions of both extraction yield and equilibrium pH. In average, the absolute
617 difference between predicted values and observed values is 0.11 in the case of the
618 yield ($MAE_{yield} = 11\%$) and 0.34 pH units for equilibrium pH ($MAE_{pH} = 0.34$). Model 2
619 additionally includes the 2:1 acid-amine complex and captures the general trend of
620 the extraction yield increase in the $0.08 - 0.3 \text{ mol L}^{-1}$ range and the subsequent
621 decline from 0.3 mol L^{-1} . Nevertheless, model 2 is unable to describe the behavior of
622 the extraction yield and equilibrium pH towards lower concentrations. The inclusion of
623 the 2:1 complex formation improved the accuracy on the estimation of the extraction
624 yield ($MAE_{yield} = 4.5\%$) but no significant improvement was observed in the
625 prediction of the pH ($MAE_{pH} = 0.33$). Model 3 includes the side reaction with water
626 soluble amines and captures correctly all the observed variations of the extraction
627 yield and equilibrium pH in all the studied concentration range. This model was more
628 accurate in the prediction of both the extraction yield ($MAE_{yield} = 2.5\%$) and the
629 equilibrium pH ($MAE_{pH} = 0.15$). This model overestimates pH for initial acid
630 concentrations between 0.008 and 0.02 mol L^{-1} . As pointed out by sensitivity
631 analysis (section 5.4), pH estimations are highly related to the considered parasite
632 reaction. The parasite reaction presented in this work is a simplification of a series of
633 acid-base reactions that could occur between acid molecules and different primary
634 amines transferred from the organic phase to the aqueous phase. Even if the
635 inclusion of the parasite reaction improved pH prediction, real phenomena are
636 expected to be more complex than those considered in the model and cause a
637 deviation from a behavior predicted using a single global pseudo-species.

638 Despite this simplification, model 3 accounted for the observed phenomena with
 639 satisfactory accuracy, in agreement with the extraction mechanism proposed in 5.2.2.
 640



641 **Figure 7.** a. Extraction yield and b. equilibrium pH as a function of initial 3-HP
 642 concentration.

643 Experimental data (symbols), model 1 (dotted line), model 2 (dashed line), model 3
 644 (solid line).

645 Error bars represent standard deviation
 646

647 Model 3 complexation constants K_{11} and K_{21} were estimated with a reasonable
 648 uncertainty (less than 10 %). The uncertainty on the reaction constant estimation K_{aq}
 649 is however higher because it represents the relatively minor side reaction of the acid
 650 with the global pseudo-species $\overline{RNH_2}$.

651

652 **Table 4.** Estimated parameters for the three proposed models

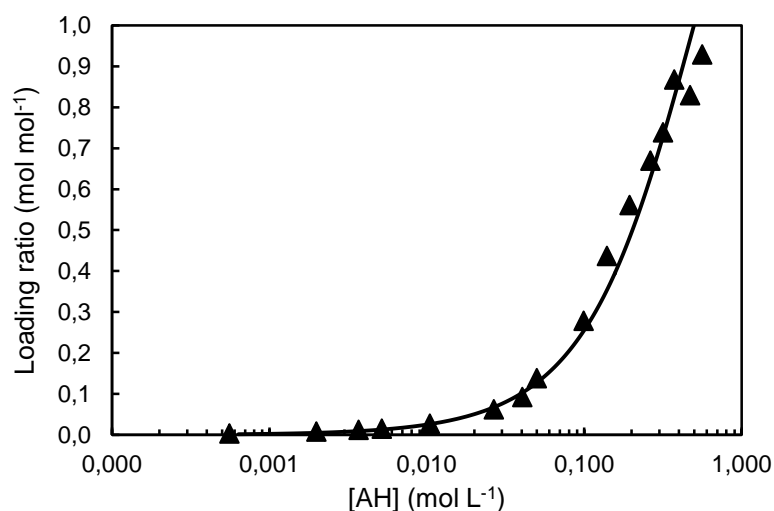
Model	Parameters	Estimated value	Coefficient* of variation, CV (%)	Model accuracy	
				MAE_{yield}	MAE_{pH}
1	K_{11} ($L^2 mol^{-2}$)	8.36×10^4	4.2%	11%	0.34
2	K_{11} ($L^2 mol^{-2}$)	5.34×10^4	5.8%	4.5%	0.33
	K_{21} ($L mol^{-1}$)	3.28	14.4%		
3**	K_{11} ($L^2 mol^{-2}$)	8.06×10^4	3.2%	2.5%	0.15
	K_{21} ($L mol^{-1}$)	1.62	8.7%		
	K_{aq} (-)	3.98	23.9%		

653 * $CV = \frac{\text{Standard error of the estimation}}{\text{estimated value}} \times 100\%$

654 ** for $[\overline{RH_2N}]_0 = 2 \times 10^{-3} \text{ mol L}^{-1}$

655
 656 Impurities showed a clear effect on the extraction yield at very low acid
 657 concentrations ($[AH]_0 < 0.02 \text{ mol L}^{-1}$) and a minor effect in the rest of the range. The
 658 inclusion of the side reaction significantly improved the prediction of the drop of the
 659 extraction yield and the gap between the predicted pH and the experimental pH at
 660 $[AH]_0 < 0.02 \text{ mol L}^{-1}$.

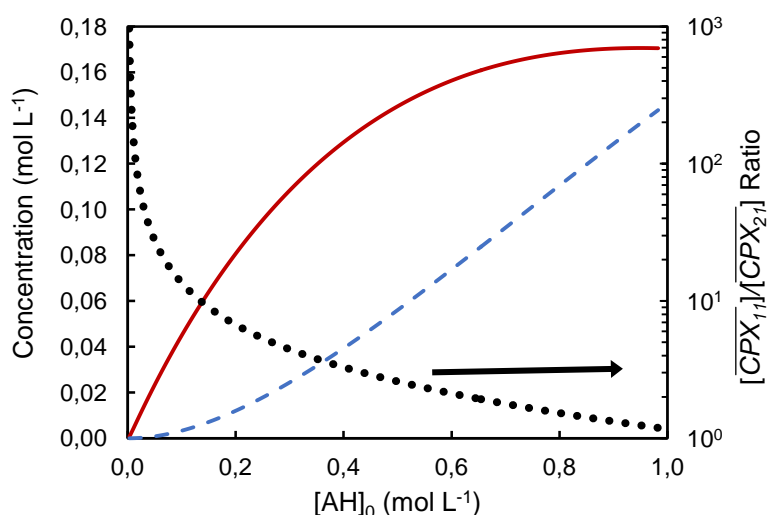
661
 662 The plot of the loading ratio as a function of the undissociated acid concentration in
 663 the aqueous phase at the equilibrium is shown in Figure 8. This curve is known as
 664 the loading curve. Experimental loading curves are generally analyzed for
 665 determining the extraction mechanisms [29]. The proposed reactive extraction model
 666 successfully predicted the loading curve, thus suggesting that model 3 accounts for
 667 the main phenomena occurring in the system.



668
 669 **Figure 8.** Loading curve of 3-HP extraction with DDMA (0.45 mol L^{-1}) in 1-dodecanol
 670 (40% v/v) and dodecane (40% v/v).
 671 Experimental (symbols), Predicted by model 3 (solid line)

672
 673 The distribution of the acid species in the organic phase calculated with model 3
 674 presented in Figure 9 is in agreement with experimental results obtained by FT-IR
 675 about the relative importance of each complexation mechanism. With model 3,
 676 $[\overline{CPX_{11}}]$ is indeed the predominant form of the acid in all the studied concentration
 677 range. The concentration of 2:1 complex $[\overline{CPX_{21}}]$ reaches the same order of

678 magnitude as $[\overline{CPX_{11}}]$ for initial acid concentrations higher than 0.13 mol L^{-1} and
 679 becomes almost equal to $[\overline{CPX_{11}}]$ at the highest acid concentration of the studied
 680 range. Experimentally, $[\overline{CPX_{21}}]$ was detected from the stretching of the carbonyl
 681 group $\nu(\text{C}=\text{O})$ for acid concentrations higher than 0.11 mol L^{-1} , thus being in
 682 accordance with the behavior depicted by the model.
 683



684 **Figure 9.** Distribution of acid species in the organic phase calculated with model 3,
 685 as a function of initial 3-HP concentration
 686
 687 Left y-axis: $[\overline{CPX_{11}}]$ (solid line), $[\overline{CPX_{21}}]$ (dashed line). Right y-axis: $[\overline{CPX_{11}}]/[\overline{CPX_{21}}]$
 688 (dotted line)

689
 690 Figure 10 presents the graphical estimation of the complexation constants from the
 691 experimental data as described in 3.6. The relative abundance of the different
 692 complexes could explain the high uncertainty on the graphical estimation of K_{21}
 693 observed in Figure 10b. The condition for yielding a straight line is $[\overline{CPX_{21}}] \gg [\overline{CPX_{11}}]$
 694 and this condition is not fulfilled in the studied range, according to Figure 9.
 695

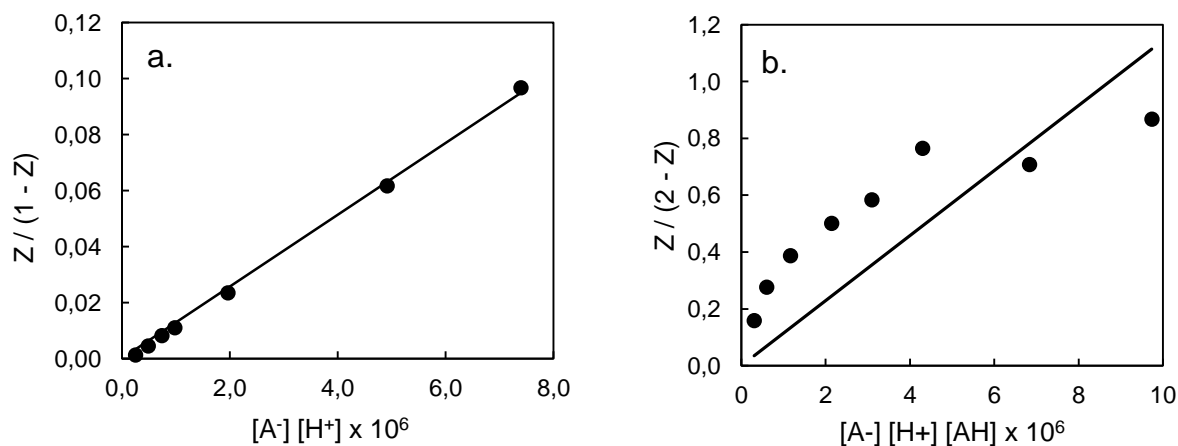


Figure 10. Graphical determination of the complexation constants K_{11} and K_{21}
 a. 1:1 ion-pair complex formation, b. 2:1 hydrogen bonded complex formation.
 Experimental data (symbols), regression line (solid line).

696
 697
 698
 699

700 Despite the high uncertainty, the relative difference of the graphically estimated
 701 values (Table 5) remains less than 10% compared to the values in Table 4 obtained
 702 by calibration of model 3.

703

704 **Table 5.** Graphically estimated complexation constants K_{11} and K_{21}

Parameter	Estimated value	Coefficient of variation [%]
K_{11} [$L^2 \text{ mol}^{-2}$]	7.645	0.87
K_{21} [$L \text{ mol}^{-1}$]	1.49	16.4

705

5.4. Sensitivity analysis of the model

706
 707

708 The goal of global sensitivity analysis is to investigate the changes of model outputs
 709 induced by modifications of model parameters. In this work, global sensitivity was
 710 evaluated using Sobol indices. Sobol indices, estimated using Monte-Carlo
 711 simulations, represent the fraction of the variance of each output that can be
 712 explained by variations of each parameter. While decomposing the variance, it is
 713 possible to estimate an effect associated to the parameter itself (main effect S_i) as
 714 well as the interaction between all the parameters. Regarding the interactions, as a
 715 matter of simplicity, a total index is defined for each parameter as the sum of its main
 716 effect and all the interactions of this parameter with the others (S_{T_i}).

717

718 The main and total Sobol indices of the parameters were estimated for two model
719 outputs: extraction yield and equilibrium pH. Only main indices are presented in this
720 section as no significant interactions between the parameters were observed. Three
721 main regions can be identified in Figure 11. Region 1 covers initial acid
722 concentrations lower than 0.02 mol L^{-1} and the variance of both outputs is mainly
723 explained by K_{11} and K_{aq} . Region 2 covers concentrations in the range 0.02 mol L^{-1} –
724 0.11 mol L^{-1} , where the variance is completely explained by K_{11} . Finally, region 3
725 covers acid concentrations above 0.11 mol L^{-1} , where K_{11} and K_{21} are the key
726 parameters explaining the variance.

727 In region 1, impurities have a moderate effect on extraction yield ($S_{K_{aq}} < 20\%$) but act
728 strongly on the equilibrium pH. Indeed, K_{aq} explains up to 85% of the variance of the
729 equilibrium pH. In this region, the ratio of estimated impurities to the initial acid is
730 equal to $0.71 \text{ mol mol}^{-1}$ for the lowest acid concentration and is equal to $0.02 \text{ mol mol}^{-1}$
731 at 0.08 mol L^{-1} . At higher acid concentrations, impurities become insignificant
732 compared to acid molecules. The considered side reaction thus significantly
733 contributes to the behavior observed at initial acid concentrations lower than 0.02 mol
734 L^{-1} .

735 In region 2, the whole variance is explained by K_{11} . This was expected because
736 $\overline{CPX_{11}}$ is the predominant form of the acid in the organic phase. As K_{21} has no
737 influence on the model outputs in regions 1 and 2, the model could be simplified to
738 1:1 complex formation plus the side reaction for initial acid concentrations below 0.11
739 mol L^{-1} .

740 When initial acid concentration exceeds 0.11 mol L^{-1} , the effect of K_{21} increases as
741 the initial 3-HP increases (region 3). This behavior is explained referring back to
742 Figure 3 and Figure 9, where it was observed that the 2:1 complex becomes
743 significant at high acid concentrations. In regions 2 and 3 the presence of primary
744 amines can be neglected, and the model could be simplified to 1:1 and 2:1 complex
745 formation without the side reaction (model 2).

746

a.

b.

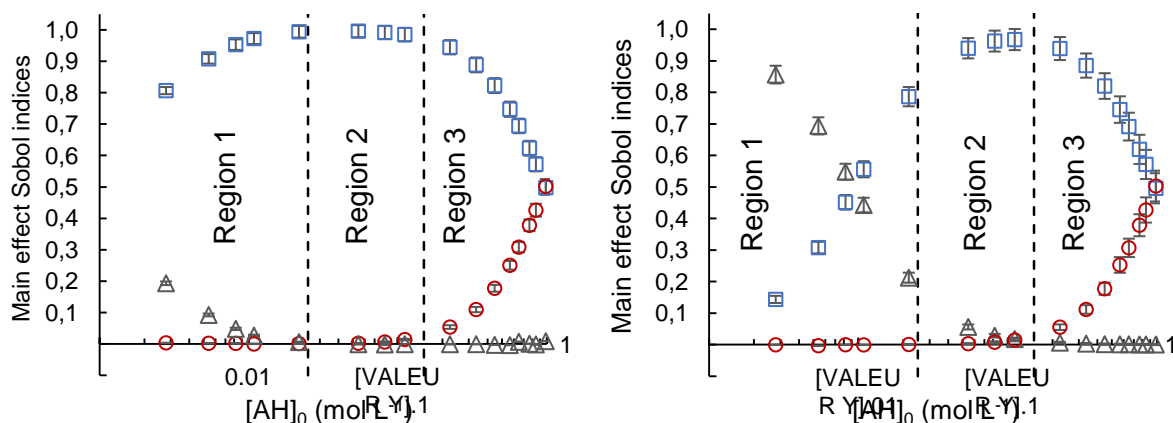


Figure 11. Sensitivity analysis of the model outputs. a. Extraction yield, b. Equilibrium pH
 K_{11} (squares), K_{21} (circles), K_{aq} (triangles)

747
748
749

750 The sensitivity analysis also explains the observations concerning the uncertainty in
 751 parameter estimation (Table 4). The equilibrium constant related to the formation of
 752 the 1:1 complex (K_{11}) has a high sensitivity for both model outputs in all
 753 concentration regions; its estimated value is thus based on the full set of
 754 measurements and has the lowest uncertainty (3.2%). The equilibrium constant
 755 related to the formation of the 2:1 complex (K_{21}) has a good sensitivity for both model
 756 outputs but in region 3 only, explaining its higher uncertainty (8.7%). As for the
 757 equilibrium constant of the side reaction (K_{aq}), its sensitivity is only significant for the
 758 pH output in region 1; the number of relevant measurements is thus small and its
 759 uncertainty the largest (23.9%).

760

761 Overall, the sensitivity analysis aligns well with the observations of sections 5.1 and
 762 5.2 about the contribution of each complexation mechanism and the uncertainty on
 763 the parameter estimation (Table 4).

764

765 6. Conclusion

766

767 In this work, we studied the reactive extraction of 3-hydroxypropionic acid with a
 768 newly designed biocompatible organic phase consisting in 20% v/v DDMA, 40% v/v
 769 1-dodecanol and 40% v/v dodecane. The loaded organic phase, analyzed by FT-IR
 770 spectroscopy, allowed to elucidate the reactive extraction mechanism of 3-HP in
 771 initial acid concentration range 0.0028 – 1 mol L⁻¹. DDMA in these diluents was found
 772 to be a stronger base than the dissociated 3-HP ($pK_{a,B} > pK_a$) being capable to bind

773 a proton from the aqueous phase. A 1:1 stoichiometry complex is then formed from
774 the interaction of the protonated amine and the dissociated acid. Besides, the 1:1
775 complex is able to extract undissociated acid molecules by the formation of hydrogen
776 bonds leading to the formation of a complex of stoichiometry 2:1. The mathematical
777 model proposed showed that the 1:1 complex predominates in all the studied
778 concentration range. The 2:1 complex becomes significant for initial acid
779 concentrations higher than 0.11 mol L^{-1} .

780

781 The extraction yield and equilibrium pH prediction were improved by taking into
782 account a side reaction related to the presence of primary amines in the organic
783 phase. The selected model successfully describes two important phenomena
784 observed experimentally at low initial 3-HP concentrations ($< 0.08 \text{ mol L}^{-1}$): poor
785 extraction yield and the underestimation of the predicted pH. The proposed model is
786 thus useful for predicting equilibrium concentrations in the studied range, which
787 corresponds to typical acid concentrations in bioconversion broths

788

789 The gained insights into reactive liquid-liquid extraction of organic acids (hereby 3-HP
790 acid), allowed to propose a methodology for mechanistic modeling that can be
791 transposed to the study of reactive liquid-liquid extraction of any particular carboxylic
792 acid of interest.

793

794 Equilibrium studies using biocompatible organic phases are essential steps for
795 developing dynamic models of ISPR processes including biological production for
796 bio-based organic acids. The development of such models will contribute to better
797 integrated bioprocess design and optimization.

798

799

800 **7. Acknowledgements**

801

802 This work was funded by a doctoral grant awarded from the ABIES doctoral school of
803 Université Paris-Saclay.

804

805

806 **8. References**

807

808 [1] C. Mcglade, P. Ekins, The geographical distribution of fossil fuels unused when
809 limiting global warming to 2 °C, *Nature*. 517 (2015) 187–190.

810 <https://doi.org/10.1038/nature14016>.

811 [2] P. Stegmann, M. Londo, M. Junginger, The circular bioeconomy : Its elements
812 and role in European bioeconomy clusters, *Resour. Conserv. Recycl.* X. 6

813 (2020) 100029. <https://doi.org/10.1016/j.rcrx.2019.100029>.

814 [3] S.K. Panda, L. Sahu, S.K. Behera, R.C. Ray, Research and production of
815 organic acids and industrial potential, *Bioprocess. Biomol. Prod.* (2019) 195–

816 209. <https://doi.org/10.1002/9781119434436.ch9>.

817 [4] S. Kumar, S. Pandey, K.L. Wasewar, N. Ak, H. Uslu, Reactive extraction as an
818 intensifying approach for the recovery of organic acids from aqueous solution:

819 a comprehensive review on experimental and theoretical studies, *J. Chem.*

820 *Eng. Data*. 66 (2021) 1557–1573. <https://doi.org/10.1021/acs.jced.0c00405>.

821 [5] K.L. Wasewar, Reactive extraction: an intensifying approach for carboxylic acid
822 separation, *Int. J. Chem. Eng. Appl.* (2012) 249–255.

823 <https://doi.org/10.7763/ijcea.2012.v3.195>.

824 [6] A.S. Kertes, C.J. King, Extraction chemistry of fermentation product carboxylic
825 acids, *Biotechnol. Bioeng.* 28 (1986) 269–282.

826 <https://doi.org/10.1002/bit.260280217>.

827 [7] T. Kurzrock, D. Weuster-botz, New reactive extraction systems for separation
828 of bio-succinic acid, *Bioprocess Biosyst. Eng.* (2011) 779–787.

829 <https://doi.org/10.1007/s00449-011-0526-y>.

830 [8] V. Inyang, D. Lokhat, Kinetic studies on propionic and malic acid reactive

831 extraction using trioctylamine in 1-decanol, *Chem. Pap.* 74 (2020) 3597–3604.

- 832 <https://doi.org/10.1007/s11696-020-01194-2>.
- 833 [9] T. Werpy, G. Petersen, Top value added chemicals from biomass Volume I —
834 Results of screening for potential candidates from sugars and synthesis gas
835 top value added chemicals from biomass, United States, 2004.
836 <https://doi.org/10.2172/15008859>.
- 837 [10] J.J. Bozell, G.R. Petersen, Cutting-edge research for a greener sustainable
838 future Technology development for the production of biobased products from
839 biorefinery carbohydrates — the US Department of Energy ’ s “ Top 10 ”
840 revisited, *Green Chem.* 12 (2010). <https://doi.org/10.1039/B922014C>.
- 841 [11] C. Jers, A. Kalantari, A. Garg, I. Mijakovic, Production of 3-hydroxypropanoic
842 acid from glycerol by metabolically engineered bacteria, *Front. Bioeng.*
843 *Biotechnol.* 7 (2019) 1–15. <https://doi.org/10.3389/fbioe.2019.00124>.
- 844 [12] F. de Fouchécour, A.K. Sánchez-Castañeda, C. Saulou-Bérion, H.É. Spinnler,
845 Process engineering for microbial production of 3-hydroxypropionic acid,
846 *Biotechnol. Adv.* 36 (2018) 1207–1222.
847 <https://doi.org/10.1016/j.biotechadv.2018.03.020>.
- 848 [13] S.S. Bhagwat, Y. Li, Y.R. Cortés-Peña, E.C. Brace, T.A. Martin, H. Zhao, J.S.
849 Guest, Sustainable production of acrylic Acid via 3-hydroxypropionic acid from
850 lignocellulosic biomass, *ACS Sustain. Chem. Eng.* 9 (2021) 16659–16669.
851 <https://doi.org/10.1021/acssuschemeng.1c05441>.
- 852 [14] F. Chemarin, M. Moussa, F. Allais, I.C. Trelea, V. Athès, Recovery of 3-
853 hydroxypropionic acid from organic phases after reactive extraction with
854 amines in an alcohol-type solvent, *Sep. Purif. Technol.* 219 (2019) 260–267.
855 <https://doi.org/10.1016/j.seppur.2019.02.026>.
- 856 [15] A.K. Sánchez-Castañeda, M. Moussa, L. Ngansop, I.C. Trelea, V. Athès,

- 857 Organic phase screening for in-stream reactive extraction of bio-based 3-
858 hydroxypropionic acid: biocompatibility and extraction performances, *J. Chem.*
859 *Technol. Biotechnol.* 95 (2019) 1046–1056. <https://doi.org/10.1002/jctb.6284>.
- 860 [16] A.D. Pérez, V.M. Gómez, S. Rodríguez-Barona, J. Fontalvo, Liquid – liquid
861 equilibrium and molecular toxicity of active and inert diluents of the organic
862 mixture tri-iso-octylamine/dodecanol / dodecane as a potential liquid membrane
863 for lactic acid removal, *J. Chem. Eng. Data.* 64 (2019) 3028–3035.
864 <https://doi.org/10.1021/acs.jced.9b00132>.
- 865 [17] G. Burgé, M. Moussa, C. Saulou-Bérion, F. Chemarin, M. Kniest, F. Allais, H.E.
866 Spinnler, V. Athès, Towards an extractive bioconversion of 3-hydroxypropionic
867 acid: study of inhibition phenomena, *J. Chem. Technol. Biotechnol.* 92 (2017)
868 2425–2432. <https://doi.org/10.1002/jctb.5253>.
- 869 [18] R. Canari, A.M. Eyal, Extraction of carboxylic acids by amine-based
870 extractants: Apparent extractant basicity according to the pH of half-
871 neutralization, *Ind. Eng. Chem. Res.* 42 (2003) 1285–1292.
872 <https://doi.org/10.1021/ie010578x>.
- 873 [19] R.R. Grinstead, J.C. Davis, Base strengths of amine-amine hydrochloride
874 systems in toluene, *J. Phys. Chem.* 72 (1968) 1630–1638.
875 <https://doi.org/10.1021/j100851a041>.
- 876 [20] M. Puttemans, L. Dryon, D.L. Massart, Extraction of organic acids by ion-pair
877 formation with tri-n-octylamine. Part 3. Influence of counter-ion and analyte
878 concentration, *Anal. Chim. Acta.* 165 (1984) 245–256.
879 [https://doi.org/10.1016/S0003-2670\(00\)85206-X](https://doi.org/10.1016/S0003-2670(00)85206-X).
- 880 [21] J.A. Tamada, C.J. King, Extraction of carboxylic acids with amine extractants.
881 2. chemical interactions and interpretation of data, *Ind. Eng. Chem. Res.* 29

- 882 (1990) 1327–1333. <https://doi.org/10.1021/ie00103a036>.
- 883 [22] D. Datta, S. Kumar, H. Uslu, Status of the reactive extraction as a method of
884 separation, *J. Chem.* 2015 (2015). <https://doi.org/10.1155/2015/853789>.
- 885 [23] A.R. Katritzky, R.L. Parris, E.S. Ignatchenko, S.M. Allin, M. Siskin, Reaction of
886 aliphatic amines with 49% formic acid . I) N,N-dimethyl-1-dodecylamine,
887 *Engineering*. 339 (1997) 59–65. <https://doi.org/10.1002/prac.19973390109>.
- 888 [24] D.R. Lide, ed., *CRC Handbook of chemistry and physics* (internet version),
889 96th ed., CRC Press, 2016.
- 890 [25] M.J.W. Jansen, Analysis of variance designs for model output, *Comput. Phys.*
891 *Commun.* 117 (1999) 35–43. [https://doi.org/10.1016/S0010-4655\(98\)00154-4](https://doi.org/10.1016/S0010-4655(98)00154-4).
- 892 [26] A. Saltelli, P. Annoni, I. Azzini, F. Campolongo, M. Ratto, S. Tarantola,
893 Variance based sensitivity analysis of model output. Design and estimator for
894 the total sensitivity index, *Comput. Phys. Commun.* 181 (2010) 259–270.
895 <https://doi.org/10.1016/j.cpc.2009.09.018>.
- 896 [27] G. Kaur, K. Elst, Development of reactive extraction systems for itaconic acid:
897 A step towards in situ product recovery for itaconic acid fermentation, *RSC*
898 *Adv.* 4 (2014) 45029–45039. <https://doi.org/10.1039/c4ra06612j>.
- 899 [28] F. Chemarin, M. Moussa, M. Chadni, B. Pollet, P. Lieben, F. Allais, I.C. Trelea,
900 V. Athès, New insights in reactive extraction mechanisms of organic acids: An
901 experimental approach for 3-hydroxypropionic acid extraction with tri-n-
902 octylamine, *Sep. Purif. Technol.* 179 (2017) 523–532.
903 <https://doi.org/10.1016/j.seppur.2017.02.018>.
- 904 [29] J.A. Tamada, A.S. Kertes, C.J. King, Extraction of carboxylic acids with amine
905 extractants. 1. equilibria and law of mass action modeling, *Ind. Eng. Chem.*
906 *Res.* 29 (1990) 1319–1326. <https://doi.org/10.1021/ie00103a035>.

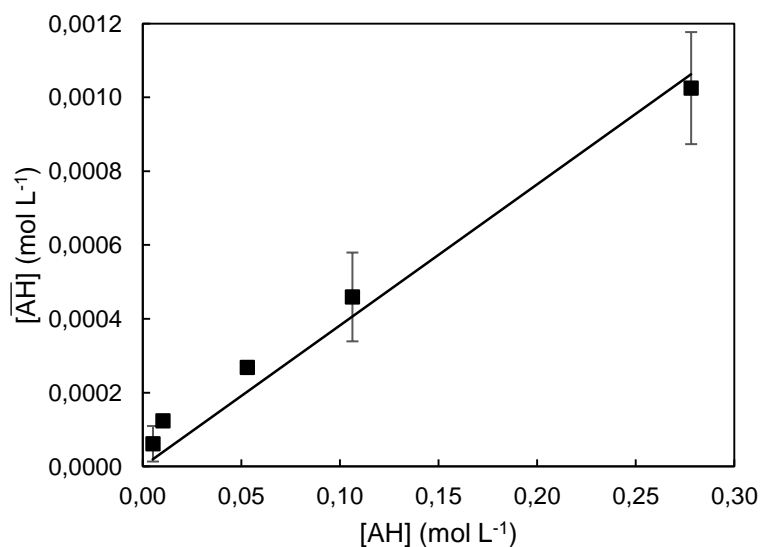
- 907 [30] D. Datta, S. Kumar, Reactive extraction of pyridine carboxylic acids with N,N-
908 dioctyloctan-1-amine: experimental and theoretical studies, *Sep. Sci. Technol.*
909 48 (2013) 898–908. <https://doi.org/10.1080/01496395.2012.712591>.
- 910 [31] J.J. Max, C. Chapados, Infrared spectroscopy of aqueous carboxylic acids:
911 comparison between different acids and their salts, *J. Phys. Chem. A.* 108
912 (2004) 3324–3337. <https://doi.org/10.1021/jp036401t>.
- 913 [32] H. Ziegenfuß, G. Maurer, Distribution of acetic acid between water and organic
914 solutions of tri-n-octylamine, *Fluid Phase Equilib.* 102 (1994) 211–255.
915 [https://doi.org/10.1016/0378-3812\(94\)87078-0](https://doi.org/10.1016/0378-3812(94)87078-0).
- 916 [33] W. Qin, Z. Li, Y. Dai, Extraction of monocarboxylic acids with trioctylamine:
917 equilibria and correlation of apparent reactive equilibrium constant, *Ind. Eng.*
918 *Chem. Res.* 42 (2003) 6196–6204. <https://doi.org/10.1021/ie021049b>.
- 919 [34] A.M. Eyal, R. Canari, pH dependence of carboxylic and mineral acid Extraction
920 by Amine-Based Extractants: Effects of pKa, Amine Basicity, and Diluent
921 Properties, *Ind. Eng. Chem. Res.* 34 (1995) 1789–1798.
922 <https://doi.org/10.1021/ie00044a030>.
- 923 [35] F. Chemarin, M. Moussa, F. Allais, V. Athès, I.C. Trelea, Mechanistic modeling
924 and equilibrium prediction of the reactive extraction of organic acids with
925 amines: A comparative study of two complexation-solvation models using 3-
926 hydroxypropionic acid, *Sep. Purif. Technol.* 189 (2017) 475–487.
927 <https://doi.org/10.1016/j.seppur.2017.07.083>.
- 928 [36] V. Inyang, D. Lokhat, Reactive extraction of malic acid using trioctylamine in 1–
929 decanol: equilibrium studies by response surface methodology using Box
930 Behnken optimization technique, *Sci. Rep.* 10 (2020) 1–10.
931 <https://doi.org/10.1038/s41598-020-59273-z>.

- 932 [37] V.R. Dhongde, B.S. De, K.L. Wasewar, Experimental study on reactive
933 extraction of malonic acid with validation by Fourier Transform Infrared
934 Spectroscopy, *J. Chem. Eng. Data.* 64 (2019) 1072–1084.
935 <https://doi.org/10.1021/acs.jced.8b00972>.
- 936 [38] N. Thakre, A.K. Prajapati, S.P. Mahapatra, A. Kumar, A. Khapre, D. Pal,
937 Modeling and optimization of reactive extraction of citric acid, *J. Chem. Eng.*
938 *Data.* 61 (2016) 2614–2623. <https://doi.org/10.1021/acs.jced.6b00274>.
- 939 [39] G. V. Gusakova, G.S. Denisov, A.L. Smolyanskii, A spectroscopic study of the
940 interaction of isobutyric acid with pyridine and dioxan, *J. Appl. Spectrosc.* 14
941 (1971) 628–632. <https://doi.org/10.1007/BF00605803>.
- 942 [40] G.M. Barrow, The nature of hydrogen bonded ion-pairs: the reaction of pyridine
943 and carboxylic acids in chloroform, *J. Am. Chem. Soc.* 78 (1956) 5802–5806.
944 <https://doi.org/10.1021/ja01603a022>.
- 945 [41] G. V. Gusakova, G.S. Denisov, A.L. Smolyanskii, Spectroscopic investigation
946 of the reaction of acetic and isobutyric acids with tertiary amines, *J. Appl.*
947 *Spectrosc.* 17 (1972) 1321–1325. <https://doi.org/10.1007/BF00940374>.
- 948 [42] J.W. Smith, M.C. Vitoria, Infrared spectroscopic investigations of acid–base
949 interactions in aprotic solvents. Part I. The interaction of tri-n-propylamine and
950 some carboxylic acids, *J. Chem. Soc. A.* (1968) 2468–2474.
951 <https://doi.org/10.1039/J19680002468>.
- 952 [43] M. Wierzejewska-Hnat, Z. Mielke, H. Ratajczak, Infrared studies of complexes
953 between carboxylic acids and tertiary amines in argon matrices, *J. Chem. Soc.*
954 *Faraday Trans. 2 Mol. Chem. Phys.* 76 (1980) 834–843.
955 <https://doi.org/10.1039/F29807600834>.
- 956 [44] J.A. Tamada, C.J. King, Extraction of carboxylic acids with amine Extractants.

957 3. effect of temperature, water coextraction, and process considerations, Ind.
958 Eng. Chem. Res. 29 (1990) 1333–1338. <https://doi.org/10.1021/ie00103a037>.
959

960 9. Appendices

961

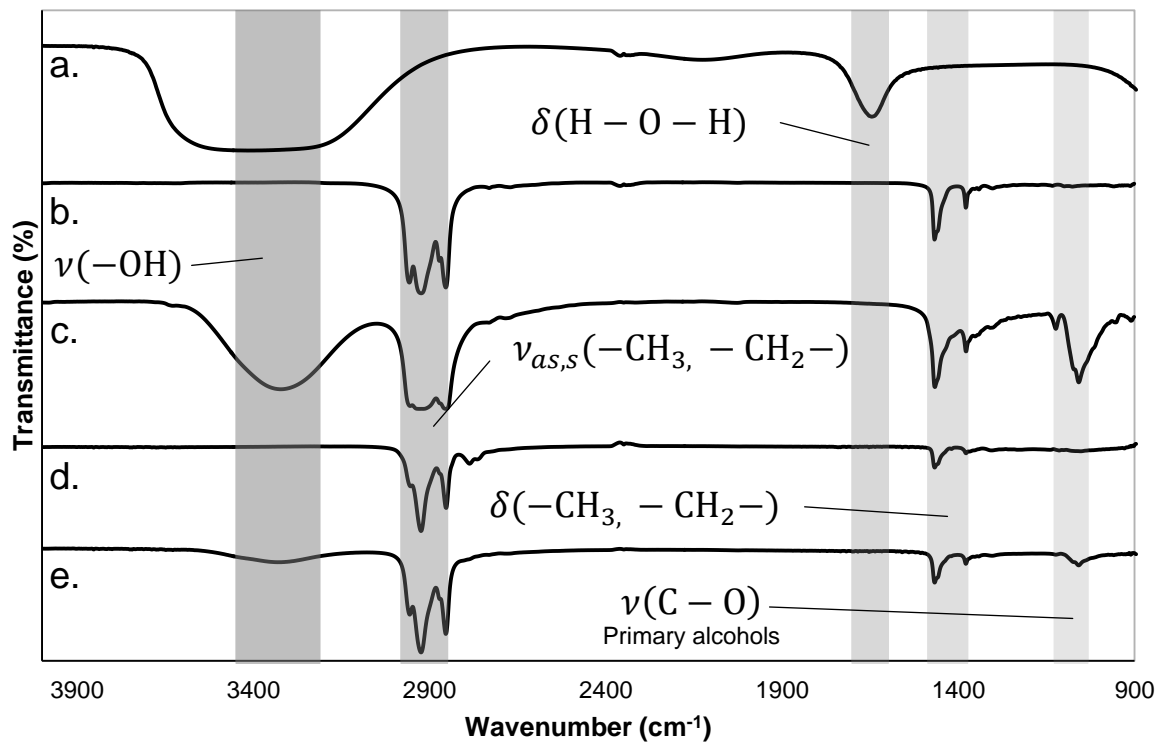


962

963

964 **Figure A1.** Estimation of physical partitioning constant K_m . Experimental data
(symbols), Regression line (solid line). Error bars correspond to standard deviation
965 ($n = 3$)
966

967



968

969

970

971

972

Figure A2. FT-IR spectra of different compounds/phases used in this study
 a. Water, b. Dodecane, c. 1-dodecanol, c. Purified DDMA, d. Organic phase (40% v/v
 1-dodecanol, 40% v/v dodecane, 20% v/v purified DDMA)